11th International Symposium on Turbulence and Shear Flow Phenomena (TSFP11)
Southampton, UK, July 30 to August 2, 2019

EFFECT OF ROUGH-SURFACE SKEWNESS ON TURBULENCE AND DRAG

Michael P. Schultz

Department of Naval Architecture & Ocean Engineering
United States Naval Academy
590 Holloway Road
Annapolis, MD 21402 USA
mschultz@usna.edu

Ralph J. Volino

Department of Mechanical Engineering
United States Naval Academy
590 Holloway Road
Annapolis, MD 21402 USA
volino@usna.edu

Karen A. Flack

Department of Mechanical Engineering
United States Naval Academy
590 Holloway Road
Annapolis, MD 21402 USA
flack@usna.edu

ABSTRACT

Previous work by the authors (Flack and Schultz, 2010) has identified the root-mean-square roughness height, k_{rms}, and the skewness, *Sk*, of the surface elevation distribution as important parameters in scaling the skin-friction drag on rough surfaces. In this study, three surfaces are tested in turbulent boundary layer flow at a friction Reynolds number, Re_τ = 1600 - 2200. All the surfaces have similar root-mean-square roughness height, while the skewness is systematically varied. Measurements are presented using both two-component LDV and PIV. The results show the anticipated trend of increasing skin-friction drag with increasing skewness. The largest increase in drag occurs going from negative skewness to zero skewness with a more modest increase going from zero to positive skewness. Some differences in the mean velocity and Reynolds stress profiles are observed for the three surfaces. However, these differences are confined to a region close to the rough surface, and the mean velocity and Reynolds stress profiles collapse away from the wall when scaled in outer variables. The turbulence structure as documented through two-point spatial correlations of velocity is also observed to be very similar over the three surfaces. These results support Townsend's (1976) concept of outer-layer similarity that the wall boundary condition exerts no direct influence on the turbulence structure away from the wall except in setting the velocity and length scales for the outer layer.

INTRODUCTION

Predicting the skin-friction drag of a generic roughness based on its surface topography is an important, yet unresolved objective in fluid mechanics research. Nikuradse (1933) carried out seminal research into roughness effects in wall-bounded turbulent flows. His study employed monodisperse, close-packed sand grains attached to the walls of a pipe. The resulting friction factor in the pipe was related to size of the sand grains used. This led to the widespread adoption of the equivalent sand roughness height, k_s, to characterize the frictional losses of all rough surfaces. Based on the research of Nikuradse (1933) and Colebrook (1939), Moody (1944) developed a practical engineering tool to predict the frictional losses in pipes. This is the well-known Moody diagram. It is difficult to overstate the impact the Moody diagram has had. For example, it is still prominently featured in undergraduate texts and used by practicing engineers some 75 years after its development. However, use of the Moody diagram requires specifying an equivalent roughness height or k_s for the surface in question, and k_s is only a physical roughness scale for uniform, close-packed sand. For all other surfaces, it is a hydraulic length scale that must be determined via numerical or physical experiment. Therefore, the ability to link the hydraulic length scale of a surface to its physical topography is not straightforward and remains the 'holy grail' of hydraulic research.

The past decade has seen tremendous interest, and progress, in better linking the physical characteristics of rough surfaces to their hydraulic impact. This has occurred on both the computational and experimental fronts. Numerical studies have been aided by both an increase in computational speed (Jimenez and Moser, 2007) and the better ability to model arbitrary wall boundary conditions (i.e. immersed boundary methods; Mittal and Iaccarino, 2005). These improvements have allowed studies at higher Reynolds numbers and over more complex roughness topography (e.g. Napoli et al., 2008; Yuan and Piomelli, 2011; Chan et al., 2015; Forooghi et al., 2017; Thakkar et al., 2017, Jelly and Busse, 2018). Experimental efforts (e.g. Flack and Schultz, 2010; Mejia-Alvarez and Christensen, 2010; Barros et al., 2018) have been assisted by techniques such as rapid prototyping which has increased in both speed and fidelity. The upshot of this is that both computational and experimental studies can now more systematically explore the parameter space of surface statistics rather than simply testing a range of unrelated surface roughness conditions.

Based on a review of the literature, Flack and Schultz (2010) concluded that while a range of topographical parameters of rough surfaces correlate significantly with the hydraulic length scale, the root-mean-square roughness height, k_{rms}, and the skewness, *Sk*, of the surface elevation distribution show the strongest correlation with k_s. In the present study, the effect of skewness is isolated by testing three surfaces with fixed k_{rms} but varying *Sk* in turbulent boundary layer flow. The effect of varying *Sk* on both drag and turbulence structure is investigated.

EXPERIMENTAL METHODS

Experiments were made in a boundary layer water tunnel facility. The test section is 2m long, 0.2m wide, and nominally 0.1m high. The lower wall is a flat plate which serves as the test wall. The upper wall is adjustable and was set for a zero streamwise pressure gradient with a freestream velocity of ~1.0ms^{-1} for all cases. The experimental facility is shown in Figure 1. Further details of the experimental facility are provided in Volino et al. (2007).

Figure 1. Boundary layer water tunnel facility.

The rough surfaces were generated mathematically so the surface statistics could be systematically altered. The current surfaces have a Gaussian range of scales with the root-mean-square roughness height held constant (k_{rms} = 350 μm). The skewness of the pdf was varied with negative, positive and zero skewness over the range -1.0 < *Sk* < +1.0. The MATLAB generated surfaces were reproduced using a high-resolution 3D printer (Objet30 Pro) with a lateral resolution of 34 μm and a vertical resolution of 16 μm. The surfaces were scanned to determine the statistics of the printed surfaces. The scanned region was measured with an optical profilometer utilizing white light interferometry (Veeco Wyco NT9100), with sub-micron vertical resolution and 3.4 μm lateral resolution. Representative scans of the three test surfaces are shown in Figure 2.

Three different plates were produced for each roughness case with dimensions of 28.0 cm by 20.3 cm in the *x* and *z* directions, respectively. The test surface was comprised of six total plates arranged in a random manner. Velocity measurements were taken 127 cm downstream from the leading edge of the roughness and 150 cm downstream of the trip. The statistics of the test surfaces are shown in Table 1.

Boundary-layer velocity measurements were obtained with a TSI FSA3500 two-component laser-Doppler velocimeter (LDV). The probe volume diameter, *d*, of the LDV is 45 μm which is $d^+ < 3$ for the measurements reported herein. Further details of the LDV system can be found in Volino et al. (2007). Velocity profiles consisted of ~50 measurement locations at varying wall-normal distances. Data were acquired at a given sampling location for 540s or until 120000 velocity realizations were made. Due to the variation in data rate with distance from the wall, the number of realizations varied from 30000 - 120000. The data were collected in coincidence mode. The flow was seeded with 2 μm silver-coated glass spherical particles.

Table 1. Rough surface statistics.

	Surface: Negative Skewness	Surface: Zero Skewness	Surface: Positive Skewness
Mean amplitude, k_a (μm)	276	280	277
Root-mean-square height, k_{rms} (μm)	350	350	350
Peak-to-trough height, k_t (μm)	3449	3244	3474
Skewness, *Sk*	-0.97	0.00	+0.98
Kurtosis, *Ku*	4.17	3.00	4.18
Effective slope, *ES*	0.40	0.44	0.40

The friction velocity, U_τ, was determined using the Clauser chart method on the mean velocity profile. U_τ was verified via the total stress method (Schultz and Flack, 2007) using the plateau in the total stress (i.e. Reynolds shear plus viscous shear in the log-layer). The values of U_τ agreed within ±2% in all cases.

Velocity field data were acquired using particle image velocimetry (PIV) at the same streamwise location as the LDV profiles. For each measurement plane, 1000 image pairs were acquired using a CCD camera with a 3320×2496 pixel array. A streamwise-wall normal plane was acquired at the spanwise centerline of the test section, and two streamwise-spanwise planes were acquired at y/δ = 0.15 and 0.40.

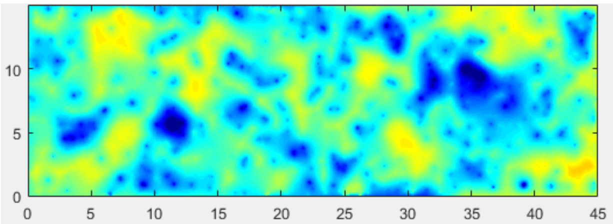

(a)

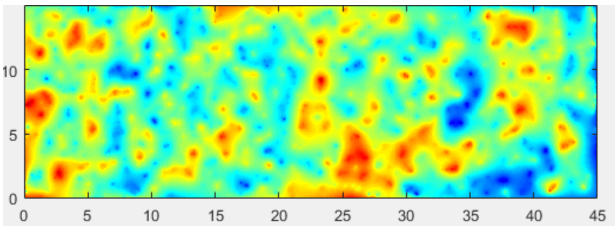

(b)

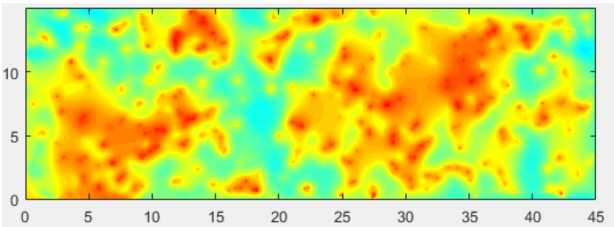

(c)

Figure 2. Scans of the test surfaces: (a) *Sk* = -1 case; (b) *Sk* = 0 case; (c) *Sk* = +1 case. Lateral dimensions are in mm. For vertical dimensions, bright red corresponds to +1.6 mm and dark blue to -1.6 mm.

RESULTS AND DISCUSSION

The experimental conditions are presented in Table 2. It can be seen that the primary effect of going from a negatively skewed roughness to a positively skewed one is an increase in the skin-friction coefficient, C_f, the boundary layer thickness, δ, and the equivalent sand roughness height, k_s. The largest increase in these quantities is observed to occur when moving from negative to zero skewness, while the increase is more modest going from zero to positive skewness. For example, the skin-friction coefficient, C_f, increases by nearly 20% between the negatively skewed and the zero skewed roughness, while the increase observed between the positively skewed and zero skewed roughness is less than 10%. This is also illustrated by the ratio of the hydraulic roughness height to the physical roughness height, k_s/k_t. The ratio k_s/k_t increases by a factor of nearly 2.5 times between the negatively skewed and the zero skewed roughness, while the increase observed between the zero skewed and positively skewed roughness is about 1.3 times. An increase in skin-friction and related quantities with increasing skewness is an expected result. However, it is worth noting that the relative magnitude of the increases seen here is quite similar to that recently observed in the numerical study of Jelly and Busse (2018). They investigated roughness topographies with only peaks, only troughs, and both peaks and troughs and found that the largest increase in skin-friction occurs going from the troughs-only surface to one with both peaks and troughs.

Table 2. Experimental conditions.

Surface	C_f ($\times 10^3$)	δ (mm)	Re_τ	k_s^+	k_s/k_t
Negative Skewness	4.65	32.2	1610	44.5	0.26
Zero Skewness	5.51	35.1	1920	114	0.64
Positive Skewness	5.94	38.4	2200	167	0.84

The mean velocity profiles are presented in Figures 3 and 4. Figure 3 shows that all the rough-wall profiles display a downward shift or roughness function, ΔU^+, compared to the smooth-wall results of Sillero et al. (2014) at similar a Reynolds number ($\delta^+ \sim 2000$). This follows the same trend with skewness as was observed in the skin-friction. Figure 4 shows the mean profiles in outer variables. Here it is seen that all of the profiles collapse in velocity-defect form supporting the notion of outer-layer similarity in the mean flow.

The majority of the roughness literature supports outer-layer similarity in the mean velocity profile. Conventional thought is that similarity can be expected to hold provided the relative roughness height (k_t/δ) is not too large. In the present work, the k_t/δ is ~10%. Connelly et al. (2006) observed outer-layer similarity in the mean flow for surfaces with a relative roughness height that was comparable to the present study. Castro (2007) asserted that mean flow universality holds for surfaces with k_t/δ up to ~20% or greater. However, recent results seem to indicate that a large relative roughness height might not be a reliable indicator for the breakdown of mean flow similarity. Instead, secondary flows can be generated on roughness with spanwise and/or streamwise periodicity, even in cases of rather small relative roughness height. Spanwise gradients in Reynolds shear stress can give rise to large-scale roll modes that lead to significant changes in the mean flow well into the outer layer and cause a breakdown in mean flow similarity (Barros and Christensen, 2014).

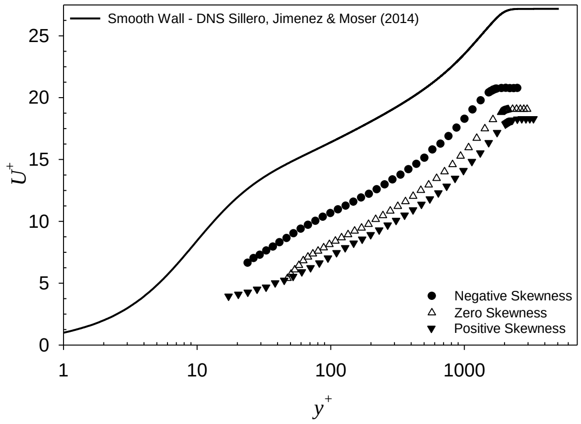

Figure 3. Mean velocity profiles in inner variables.

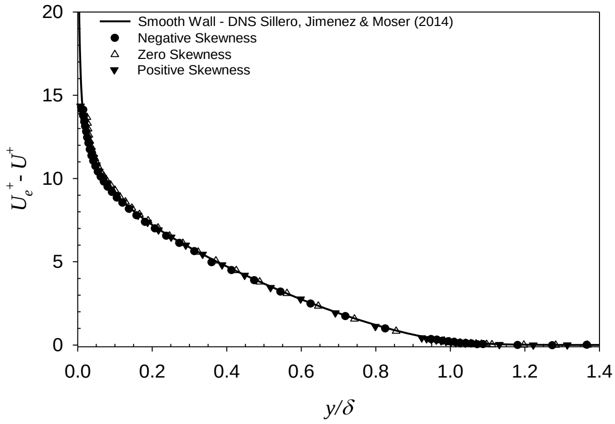

Figure 4. Mean velocity profiles in velocity-defect form.

The Reynolds stress profiles are presented in Figures 5-7. The streamwise Reynolds normal stress (u') profiles (Figure 5) indicate that the primary effect of the roughness is to suppress the near-wall peak in u' that occurs on the smooth wall. This observation is in agreement with the results of Ligrani and Moffat (1986). Their results showed a gradual reduction in the near-wall peak in u' with increasing roughness Reynolds number until the fully-rough regime is reached where a near total destruction in the peak is observed. The roughness Reynolds number range ($45 \leq k_s^+ \leq 167$) and the destruction of the near-wall peak in u' indicates that the present cases are in the fully-rough flow regime or nearly so. Differences in the profiles of u' for the rough walls are limited to $y/\delta < 0.1$, which corresponds to about one roughness height (k_t) from the wall. Farther from the wall, the profiles collapse and agree within experimental uncertainty with the smooth-wall profile of Sillero et al. (2014) at similar a Reynolds number.

The wall-normal Reynolds normal stress (v') profiles for the rough walls (Figure 6) show collapse across most of the boundary layer. Very close to the roughness ($y/\delta < 0.05$), v' appears to be enhanced for the positively skewed roughness. The present rough-wall results also agree quite well with the smooth-wall experimental results of DeGraaff and Eaton (2000) taken at a similar Reynolds number. The present rough-wall results and the smooth-wall results of DeGraaff and Eaton, acquired via LDV, lie systematically above the Sillero et al.

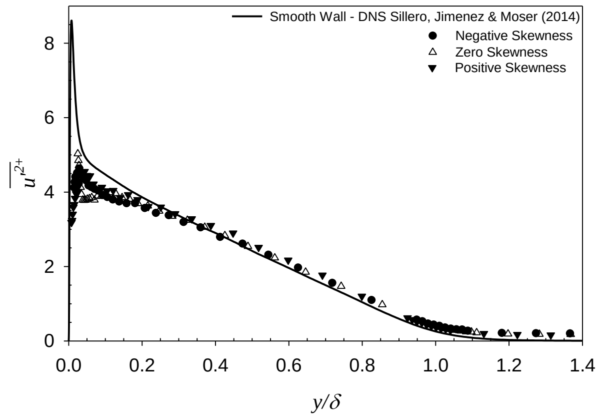

Figure 5. Streamwise Reynolds normal stress in outer variables.

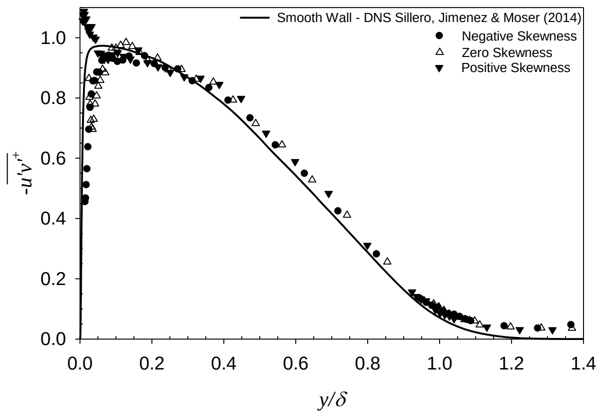

Figure 7. Reynolds shear stress in outer variables.

(2014) results as one gets farther from the wall and the freestream is approached. Since the freestream turbulence level in both the present study and the work of DeGraaff and Eaton is quite low, the fact that the wall-normal Reynolds normal stress does not go to zero in the freestream cannot be physical. This systematic overestimation of turbulence in the freestream with LDV was previously noted by DeGraaff (1999). DeGraaff hypothesized the error to be due to a slight fringe aberration resulting from the small probe volume. He showed compelling evidence that this aberration leads to overestimation of the turbulence when the turbulence intensity is low (i.e. in the freestream), but it becomes negligible when the actual turbulence intensity is increased (i.e. in the boundary layer). Therefore, this effect is expected to influence only measurements near the outer edge of the boundary layer and in the freestream and not those taken deeper in the boundary layer.

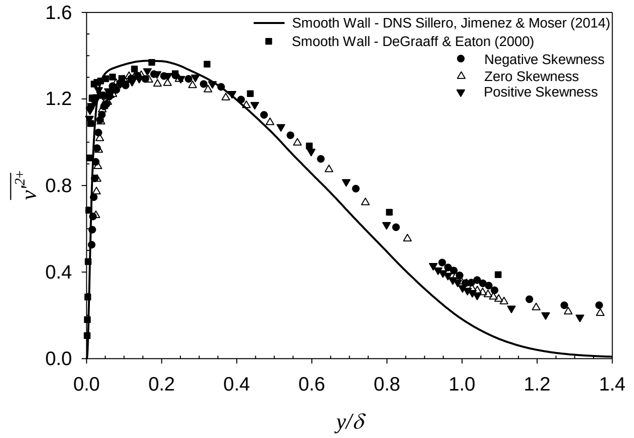

Figure 6. Wall-normal Reynolds normal stress in outer variables.

The Reynolds shear stress (*RSS*) profiles for the rough walls (Figure 7) also collapse across most of the boundary layer. Very near the roughness ($y/\delta < 0.05$), the *RSS* appears to be enhanced for the positively skewed roughness as compared to the other cases. The present rough-wall results also agree within experimental uncertainty with the smooth-wall DNS results of Sillero et al. (2014) throughout most of the boundary layer.

Figure 8 shows results from PIV taken in the streamwise-wall-normal plane. Specifically, the two-point correlations, R_{uu}, taken at y/δ=0.15 are presented.

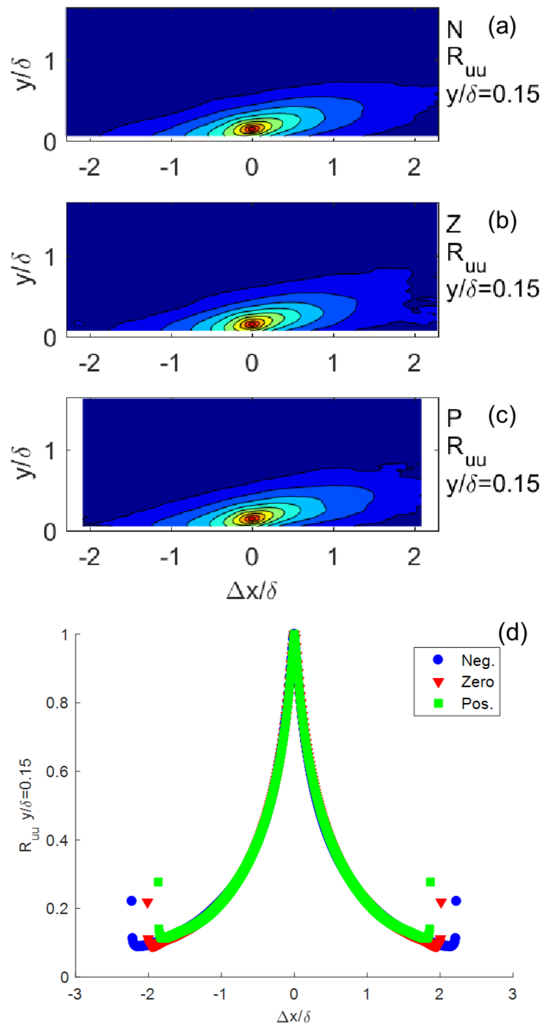

Figure 8. Two-point correlation, R_{uu}, in the streamwise-wall-normal plane centered at y/δ=0.15 for: (a) *Sk* = -1 case; (b) *Sk* = 0 case; (c) *Sk* = +1 case; (d) correlation cuts taken in streamwise direction at y/δ=0.15.

Figure 8(a-c) shows that the overall shape of the correlations for all of the rough surfaces is very similar. They also show characteristics of the same correlations taken on a smooth wall. For example, the correlations are elongated in the streamwise direction and are inclined at an angle of 10º to 15º to the wall. This is indicative of the hairpin packet vortical structure presented by Adrian et al. (2000). Figure 8(d) shows correlation cuts taken in streamwise direction at $y/d=0.15$. It can be seen that the correlations not only look similar but are also in excellent quantitative agreement.

Figure 9 shows results from PIV taken in the streamwise-spanwise plane at $y/\delta=0.15$. Two-point correlations, R_{uu}, are presented. The overall shape of the correlation maps (Figures 9(a-c)) for the three rough surfaces again look to be quite similar. Spanwise cuts (Figure 9(d)) of the correlations maps indicate that these correlations are in close agreement for the three rough surfaces.

CONCLUSION

An experimental study was conducted in which the roughness height was fixed while the skewness was systematically varied in turbulent boundary layer flow at a friction Reynolds number, $Re_\tau = 1600 - 2200$. The results show the expected trend of increasing skin-friction drag and other drag-related variables with increasing skewness. The largest increase is observed to occur going from negative to zero skewness with a more modest increase going from zero to positive skewness. This result agrees well with the recent numerical study of Jelly and Busse (2018). Also, some differences in the mean velocity and Reynolds stress profiles are observed for the three surfaces. However, these differences are found to be confined to a region within one roughness height (k_t) of the wall, and the profiles collapse farther away from the wall when scaled in outer variables. Two-point spatial correlations also indicate that the turbulence structure in the outer layer is not affected by the skewness of the roughness. The present results support Townsend's (1976) concept of outer-layer similarity that asserts that details of the wall boundary condition have no direct influence on the turbulence structure away from the wall except in setting the velocity and length scales for the outer flow. However, it should be stressed, in light of recent studies (e.g. Barros and Christensen, 2014), that rough surfaces that exhibit significant spanwise and/or streamwise periodicity may cause outer layer similarity to break down even in cases where the relative roughness height is small.

ACKNOWLEDGEMENTS

The authors would like to acknowledge the U.S. Office of Naval Research for financial support of this work. The assistance of the Naval Academy Hydromechanics Lab and the Project Support Branch is also gratefully acknowledged.

REFERENCES

Adrian, R. J., Meinhart, C. D., and Tompkins, C. D., 2000, "Vortex Organization in the Outer Region of the Turbulent Boundary Layer", *Journal of Fluid Mechanics,* Vol. 422, pp. 1-54.

Barros, J. M. and Christensen, K. T., 2014, "Measurements of Skin-friction of Systematically Generated Surface Roughness", *Journal of Fluid Mechanics*, Vol. 748, pp. R1-1-R1-13.

Barros, J. M., Schultz, M. P., and Flack, K. A., 2018, "Measurements of Skin-friction of Systematically Generated Surface Roughness", *International Journal of Heat and Fluid Flow*, Vol. 72, pp. 1-7.

Castro, I. P., 2007, "Rough-wall Boundary Layers: Mean Flow Universality", *Journal of Fluid Mechanics*, Vol. 585, pp. 469-485.

Chan, L., MacDonald, M., Chung, D., Hutchins, N., and Ooi, A., 2015, "A Systematic Investigation of Roughness Height and Wavelength in Turbulent Pipe Flow in the Transitionally Rough Regime", *Journal of Fluid Mechanics*, Vol. 771, pp. 743-777.

Colebrook, C. F., 1939, "Turbulent Flow in Pipes, with Particular Reference to the Transitional Region between Smooth and Rough Wall Laws", *Journal of the Institution of Civil Engineers*, Vol. 11, pp. 133-156.

Connelly, J. S., Schultz, M. P., and Flack, K. A., 2006, "Velocity-defect Scaling for Turbulent Boundary Layers with a Range of Relative Roughness", *Experiments in Fluids*, Vol. 40, pp. 188-195.

DeGraaff, D. B., 1999, *Reynolds Number Scaling of the Turbulent Boundary Layer on a Flat Plate and on Swept and Unswept Bumps*, Ph.D. Dissertation, Stanford University, Stanford, CA.

DeGraaff, D. B. and Eaton, J. K., 2000,"Reynolds-number Scaling of the Flat-plate Turbulent Boundary Layer", *Journal of Fluid Mechnaics*, Vol. 422, pp. 319-346.

Flack, K. A. and Schultz, M. P., 2010, "Review of Hydraulic Roughness Scales in the Fully Rough Regime", *AMSE Journal of Fluids Engineering*, Vol. 132, Art. No. 041203, 10 pp.

Forooghi, P., Stroh, A., Magagnato, F., Jakirlic, S., and Frohnapfel, B., 2017, "Towards a Universal Roughness Correlation," *AMSE Journal of Fluids Engineering*, Vol. 139, Art. No. 121201, 12 pp.

Jelly, T. O. and Busse, A., 2018, "Reynolds and Dispersive Shear Stress Contributions above Highly Skewed Roughness", *Journal of Fluid Mechnaics*, Vol. 852, pp. 710-724.

Jimenez, J. and Moser, R. D., 2007, "What are We Learning from Simulating Wall Turbulence?", *Philosophical Transactions of the Royal Society A*, Vol. 365, pp. 715-732.

Ligrani, P. M. and Moffat, R. J., 1986, "Structure of Transitionally Rough and Fully Rough Turbulent Boundary Layers", *Journal of Fluid Mechanics*, Vol. 162, pp. 69-98.

Mejia-Alvarez, R. and Christensen, K. T., 2010, "Low-order Representations of Irregular Surface Roughness and Their Impact on a Turbulent Boundary Layer", *Physics of Fluids*, Vol. 22, Art. No. 015106, 20 pp.

Mittal, R. and Iaccarino, G., 2005, "Immersed Boundary Methods", *Annual Review of Fluid Mechanics*, Vol. 37, pp. 239-261.

Moody, L. F., 1944, "Friction Factors for Pipe Flow", *Transactions ASME*, Vol. 66, pp. 671-684.

Napoli, E., Armenio, V., and De Marchis, M., 2008, "The Effect of the Slope of Irregularly Distributed Roughness Elements on Turbulent Wall-bounded Flows", *Journal of Fluid Mechanics*, Vol. 613, pp. 385-394.

Nikuradse, J., 1933, "Laws of Flow in Rough Pipes", *NACA Tech. Memo*. 1292.

Schultz, M. P. and Flack, K. A., 2007, "The Rough-wall Turbulent Boundary Layer from the Hydraulically Smooth to the Fully Rough Regime", *Journal of Fluid Mechanics*, Vol. 580, pp. 381-405.

Sillero, J. A., Jimenez, J., and Moser, R. D., 2014, "Two-point Statistics for Turbulent Boundary Layers and Channels at Reynolds Numbers up to $\delta^+ \approx 2000$", *Physics of Fluids*, Vol. 26, Art. No. 105109, 30 pp.

Thakkar, M., Busse, A., and Sandham, N., 2017, "Surface Correlations of Hydrodynamic Drag for Transitionally Rough Engineering Surfaces", *Journal of Turbulence*, Vol. 18, pp. 138-169.

Townsend, A. A., 1976, *The Structure of Turbulent Shear Flow*, Cambridge University Press, 2nd Edition.

Volino, R. J., Schultz, M. P., and Flack, K. A., 2007, "The Turbulence Structure in Rough- and Smooth-Wall Boundary Layers", *Journal of Fluid Mechanics*, Vol. 592, pp. 263-293.

Yuan, J. and Piomelli, U., 2011, "Estimation and Prediction of the Roughness Function of Realistic Surfaces", *Journal of Turbulence*, Vol. 15, pp. 350-365.

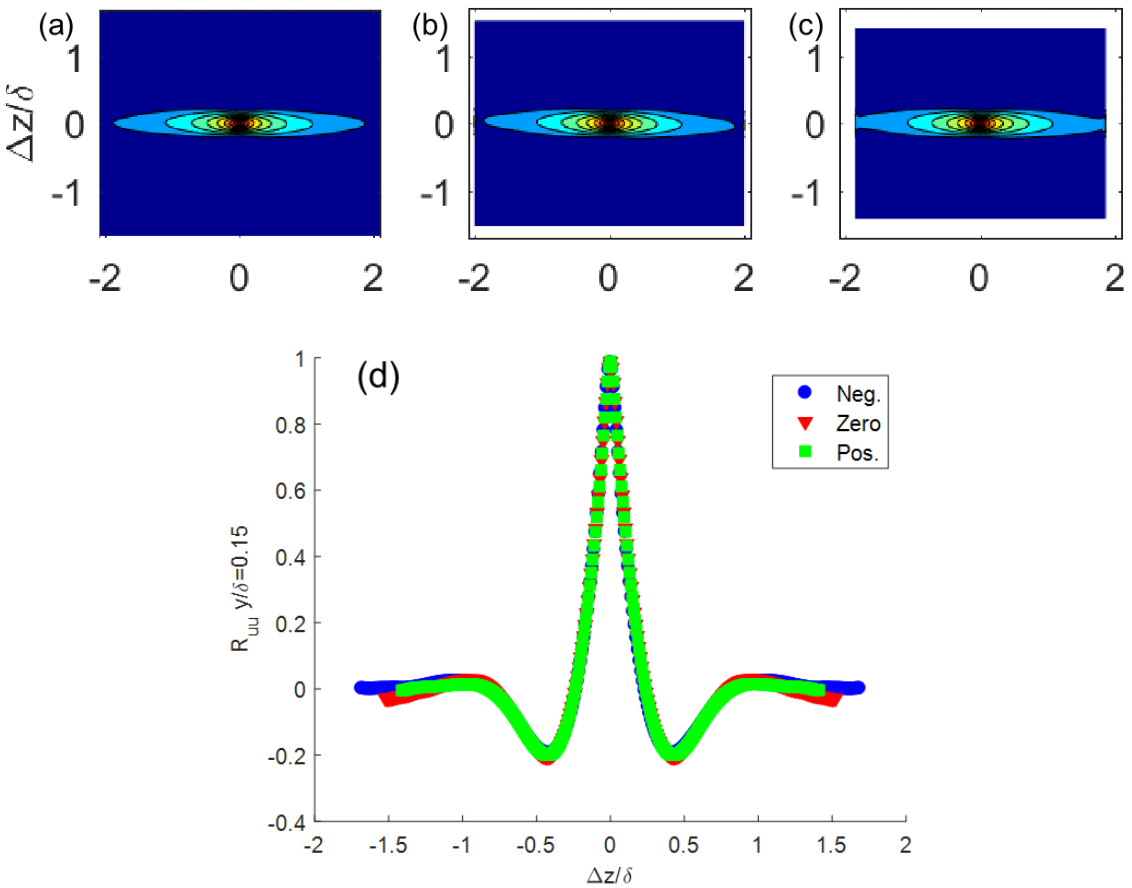

Figure 9. Two-point correlation, R_{uu}, in the streamwise-spanwise plane centered at y/δ=0.15 for: (a) Sk = -1 case; (b) Sk = 0 case; (c) Sk = +1 case; (d) correlation cuts taken in the spanwise direction at y/δ=0.15.